Chemistry–A European Journal
Research Article
doi.org/10.1002/chem.202402106
Chemistry Europe
European Chemical Societies Publishing
www.chemeurj.org

Effects of Ring Functionalization in Anthracene-Based Cyclophanes on the Binding Properties Toward Nucleotides and DNA

Ismet Basaran,[a] Aleksandr M. Agafontsev,[a] Boris S. Morozov,[a] Alexander S. Oshchepkov,[b] Petra Imhof,[c] and Evgeny A. Kataev*[a]

Supramolecular recognition of nucleobases and short sequences is an emerging research field focusing on possible applications to treat many diseases. Controlling the affinity and selectivity of synthetic receptors to target desired nucleotides or short sequences is a highly challenging task. Herein, we elucidate the effect of substituents in the phenyl ring of the anthracene-benzene azacyclophane on the recognition of nucleoside triphosphates (NTPs) and double-stranded DNA. We show that introducing phenyl rings increases the affinity for NTPs 10-fold and implements groove and intercalation binding modes with double-stranded DNA. NMR studies and molecular modeling calculations support the ability of cyclophanes to encapsulate nucleobases as part of nucleotides.

Introduction

The study of non-covalent interactions of synthetic receptors with biologically important targets in aqueous solution is essential for understanding and mimicking nature. Artificial systems will permit the development of new drug candidates, delivery agents, and diagnostic agents.[1] Water-soluble cyclophanes are promising supramolecular hosts for the recognition of nucleobases and derivatives.[2] They have been shown to form complexes with nucleotides,[2g,3] bind to double-stranded DNA,[3b,4] RNA,[5] recognize abasic sites and mismatched base pairs,[6] and even show moderate sequence selectivity.[7] For instance, acyclic anthracene-based structures developed by Kumar show a preference to bind poly(dG-dC) over poly(dA-dT) via intercalation.[8,9] A family of azacyclophanes was recently studied by Granzhan and Teulade-Fichou in the detection of mismatched thymine residues in the duplex DNA structure.[10] The nature of the aromatic ring and the position of the attachment to the spacers were found to determine the selectivity in the mismatch recognition.[11] Styrylpyridine-based cyclophanes developed by Ihmels and co-workers were found to bind and detect pyrimidine nucleotides.[12] These investigations suggest that variations in the structure of the cyclophane receptor have a dramatic effect on recognition and sensing properties. However, for a systematic understanding of the structure-property relationship, cyclophanes bearing two different π-systems with the possibility to vary functional groups on them could be perfect models. In this work, we design such a system and explore the effect of substitution in the rings of the anthracene-based cyclophanes on the binding properties of the receptors toward nucleotides and double-stranded DNA sequences. The results clue up the structure-property relationship and approaches to designing the receptors with the desired binding ability and fluorescent properties.

To this end, we have synthesized three new azacyclophanes with phenyl rings extending the π-surface to bind nucleobases via π-π interactions efficiently. The bottom and the top π-systems in the cyclophane are connected through an aza-spacer, 2-(2-aminoethoxy)ethylamine, which are positively charged in water and provide electrostatic attraction to bind nucleotides. The results reveal a dramatic influence of an additional phenyl ring on the binding properties. The cyclophane with a phenyl group placed in the *ortho*-position to the aminomethyl linkers showed at least 10-fold higher affinity for nucleoside triphosphates than the other two cyclophanes. However, the *meta*-substituted analog demonstrated selectivity for GC motifs in the double-stranded DNA (dsDNA) binding experiments. Excimer formation in the presence of dsDNA was found for the unsubstituted cyclophane, indicating its ability to fit into the major groove. The molecular dynamics simulations also confirmed major groove and intercalation binding modes with DNA.

[a] *I. Basaran, A. M. Agafontsev, B. S. Morozov, E. A. Kataev*
Department of Chemistry and Pharmacy, Friedrich-Alexander University (FAU) Erlangen-Nürnberg, 91052 Erlangen, Germany
E-mail: evgeny.kataev@fau.de

[b] *A. S. Oshchepkov*
Organic Chemistry Department, Institute of Chemistry Martin-Luther-University Halle-Wittenberg, Kurt-Mothes-Straße 2, 06120 Halle, Germany

[c] *P. Imhof*
Computer Chemistry Center, Department of Chemistry and Pharmacy, Friedrich-Alexander University (FAU) Erlangen-Nürnberg, 91052 Erlangen, Germany

Supporting information for this article is available on the WWW under https://doi.org/10.1002/chem.202402106

Results and Discussion

We proposed connecting the anthracene and the benzene rings through the 2-(2-aminoethoxy)ethylamine linker to design the cyclophanes that can be functionalized at the top ring – benzene ring. The synthesis of the first receptor PA was accomplished by using 2,5-benzene-dicarboxaldehyde (Figure 1). The introduction of the bromo-substituent in the dialdehyde structure allows one to attach various functional groups, including additional aromatic rings, via Pd-coupling reactions. Therefore, we introduced phenyl substituents into the dialdehyde to obtain two new cyclophanes with *ortho*– (*o*-Ph-PA) and *meta*–substituted rings (*m*-Ph-PA) relative to the spacer connection. The receptors were synthesized from the corresponding dialdehydes and the anthracene derivative bearing two spacer arms, as shown in Figure 1. The latter was prepared by the condensation of mono-BOC-protected 2-(2-aminoethoxy)ethylamine with anthracene-9,10-dicarboxaldehyde followed by the reduction of the imine bonds and BOC-group deprotection (*cf.* SI). For the preparation of the phenyl-substituted cyclophanes, we used the corresponding dialdehydes bearing a phenyl group in the *ortho*– or *meta*–positions.[13] The macrocyclic formation was achieved in moderate yields 20–33 %.

The pH-dependent fluorescence experiments showed average pK_a values of 5.7 for all three cyclophanes (Figure S6). This value is in accordance with the previously reported anthracene- and pyrene-based cyclophanes.[2f,g] We investigated the binding properties of the cyclophanes in a 50 mM MES buffer, pH 6.2 (2 % DMSO). At this pH, the cyclophanes are present in solution in 3- and 4-fold protonated states.[2g] Molecular structures of the 4-fold protonated receptors were obtained by the DFT calculations performed using ORCA 5.0 software package[14] utilizing the atom-pairwise dispersion correction with the Becke-Johnson damping scheme[15] and SMD solvation module.[16] The optimized structures (Figure 1) show that the ring position can determine the overall stacking area with the encapsulated nucleobase. The conformation and shape of *m*-Ph-PA and *o*-Ph-PA are different, which should be reflected in different binding properties with oligonucleotides.

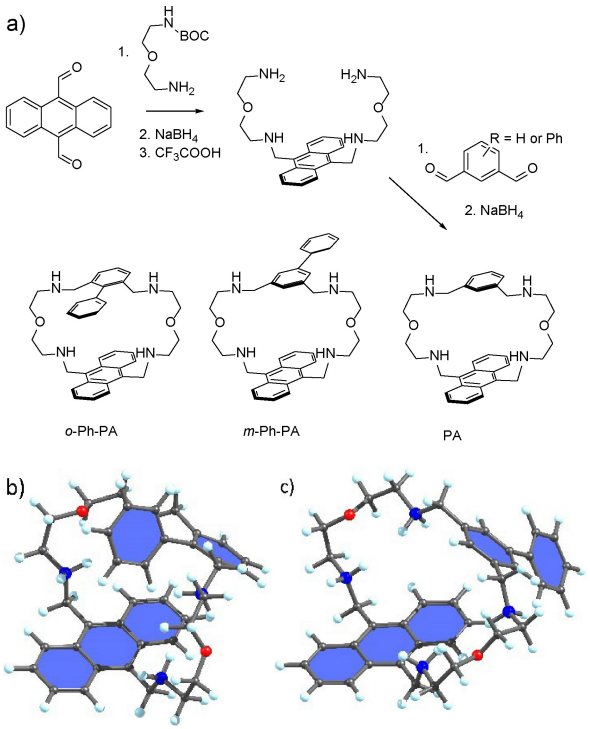

Figure 1. a) Synthesis of the investigated cyclophanes. Structures of the 4-fold protonated cyclophanes b) *o*-Ph-PA and c) *m*-Ph-PA according to the DFT calculations. BOC – tert-butyloxycarbonyl protecting group.

The association constants of host-guest complexes with nucleotides were determined by the steady-state UV-Vis, NMR and fluorescence measurements (Table 1). UV-Vis spectral changes for the three cyclophanes have specific features. *o*-Ph-PA shows the same bathochromic shift in the presence of nucleotides as PA. However, *m*-Ph-PA demonstrated hypsochromic shift, implying a different coordination mode (Figure 2a–c). Fitting analysis and Job plots experiments suggest 1:2 receptor-nucleotide stoichiometry. The second binding is weaker by more than two orders of magnitude but is still detectable. This second binding event can originate from the strong electrostatic contribution to the formation of the complex between 4-fold protonated receptor[2g] and 2/3-fold negatively charged triphosphate at pH 6.2.[17] Analysis of Table 1 reveals that *o*-Ph-PA shows almost one order of magnitude higher binding constants than PA and m-PA. The extension of the π-system in the ortho position likely imitates another anthracene ring, and thus, the overall π-surface area is increased, leading to an increase in affinity.

The shift in absorption upon nucleotide recognition suggests the interaction of a nucleobase with π-systems in the cyclophane. We conducted NMR titrations to obtain more information on how nucleotides interact with receptors. In all experiments, anthracene signals undergo upfield shifts, while ATP signals shift in lower field (approx. 0.6 ppm, Figure 2e). In a separate experiment, we found that the addition of HCl to protonate the receptors leads to downfield shift of proton signals (Figure S10). These experiments suggest that the observed shifts with nucleotides do not originate from the complexation-induced protonation but rather from direct π-π interactions. We also tested pyrophosphate as a control compound without a nucleobase, and it did not induce substantial changes in UV and NMR experiments. Interestingly,

Table 1. Apparent binding constants ($\log K_{11}$; $\log K_{12}$) for three receptors (0.01 mM) as determined from UV-Vis titrations in a 50 mM MES buffer (pH 6.2) containing 2 % DMSO.

Receptor[a]	ATP	GTP	CTP	TTP
PA	4.54 ± 0.02; 2.89 ± 0.01	4.48 ± 0.02; 2.78 ± 0.01	4.35 ± 0.02; 3.08 ± 0.01	4.15 ± 0.02; 2.65 ± 0.01
o-Ph-PA	5.99 ± 0.03; 3.84 ± 0.01	5.91 ± 0.02; 3.87 ± 0.01	5.88 ± 0.02; 3.12 ± 0.01	5.75 ± 0.02; 3.27 ± 0.01
m-Ph-PA	4.36 ± 0.02; 2.58 ± 0.01	4.538 ± 0.02; 2.94 ± 0.01	5.20 ± 0.02; 3.60 ± 0.01	4.08 ± 0.02; 2.09 ± 0.01

[a] Experiments were done in duplicate. Experimental errors are provided.

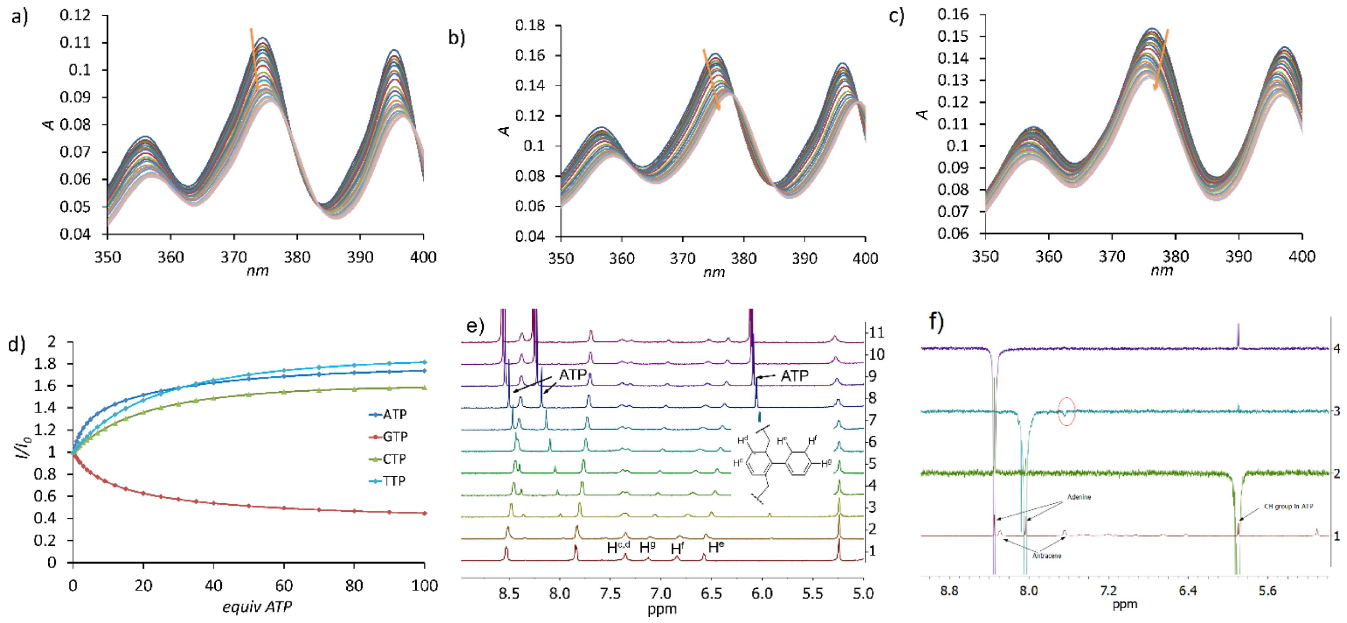

Figure 2. UV vis titration of receptors with ATP: a) PA; b) *o*-Ph-PA and c) *m*-Ph-PA. d) Fluorescence changes observed by the gradual addition of nucleotides to *o*-Ph-PA, excitation at 375 nm, slit 2/2. e) ^{1}H NMR titration of PA with ATP in a 1:1 DMSO-d6, D_2O MES buffer (pH 6.2). f) NOE experiment for *o*-Ph-PA conducted in the presence of 5 equiv. of ATP, the corresponding resonance of the anthracene protons is shown in a red circle.

the signals of the phenyl rings start to split into separated signals upon ATP addition, suggesting a direct interaction of adenine with aromatic rings and rigidification of the cyclophane structure (Figure S12). Direct evidence of adenine-anthracene interactions was obtained from NOE (Nuclear Overhauser Effect) experiments of the mixture of *o*-Ph-PA with 5 equiv. of ATP. As can be seen in Figure 2f, the saturation of one of the adenine signals leads to the response in the anthracene protons, while benzyl protons have a very weak response. All these experiments support the proximity of the adenine and anthracene rings in the complex, suggesting the encapsulation of the adenine between the π-systems in the cyclophane.

Next, we investigated how cyclophanes interact with short double-stranded DNA. For this purpose, we chose four dodecamers bearing either GC or AT repeating base pairs. Two of these dodecamers bear GC and AT base pairs in the center of the sequence: $d(CATGGGCCCATG)_2$ (G3C3) and $d(CGCAAATTTGCG)_2$ (A3T3), and the other two consist of only AT or GC base pairs: d(TATAAATTTATA), d(CGCGGGCCCGCG). The studies with nucleoside triphosphates showed that the interaction with guanine leads to quenching of fluorescence, while adenine induces a fluorescence enhancement. Therefore, the titration experiments with sequences can uncover the preference of receptors to bind either GC or AT base pairs. The addition of d(TATAAATTTATA) to the receptors resulted in fluorescence enhancement, while d(CGCGGGCCCGCG) induced quenching of the fluorescence (Figure S9). This observation is in accordance with the response observed for nucleoside triphosphates. More complex fluorescence changes were found for A3T3 and G3C3 oligonucleotides. Since the receptors are positively charged, they were expected to bind in the center of the sequences that have stronger negative charge density. As can be seen in Figure 3a this was not always the case. For instance, *o*-Ph-PA titrated with A3T3 and G3C3 showed, as expected, an enhancement and quenching of fluorescence, respectively. This behavior suggests that the receptors bind in the center of the sequence either to AT or GC base pairs. However, PA and *m*-Ph-PA demonstrated quenching followed by fluorescence enhancement in the case of A3T3 addition. We interpreted these changes as a preference of *m*-Ph-PA to bind GC base pairs. Fluorescence binding studies with four dodecamers confirmed our interpretations of the above described results. According to the obtained data, the cyclophanes are bound to the sequences in 2:1 (receptor: sequence) and 1:1 stoichiometry. The complexes with these stoichiometry were observed in ESI-MS spectra (Figure S15, S16). As can be inferred from Table 2, m-Ph-PA has an overall higher affinity to all sequences, showing the strongest affinity for d(CGCGGGCCCGCG) with $\log K_{21} = 13.0$.

Table 2. Stability constants ($\log K_{21}$; $\log K_{11}$) for three receptors (0.01 mM) as determined from UV-Vis titrations in a 50 mM MES buffer (pH 6.2) containing 2% DMSO. 2:1 stoichiometry corresponds to the coordination of two molecules of cyclophane per dsDNA sequence.

Sequence[a]	PA	*o*-Ph-PA	*m*-Ph-PA
d(CGCAAATTTGCG)	10.01; 5.50	11.31; 6.14	11.95; 6.43
d(CATGGGCCCATG)	10.06; 5.95	11.96; 5.02	11.98 [b]
d(TATAAATTTATA)	11.69; 5.63	11.09; 4.91	12.76; 6.40
d(CGCGGGCCCGCG)	10.22; 5.69	10.60; 5.03	13.00; 7.20

[a] The experimental errors do not exceed 5%. [b] not detected.

We conducted CD measurements to reveal further information on the binding mode of three cyclophanes to double-stranded DNA. For this purpose, we utilized calf thymus DNA, as

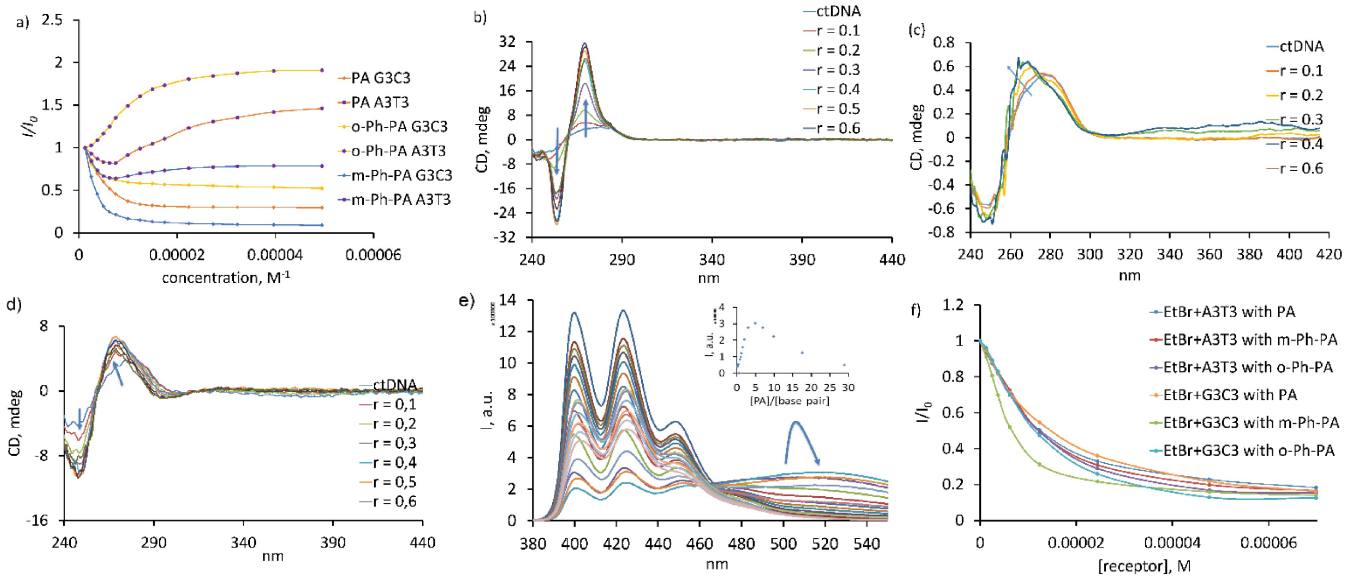

Figure 3. a) Fluorescence changes induced by the addition of G3C3 and A3T3 sequences to the receptor solution (excitation at 375 nm, slit 2/2). CD titration of ctDNA with b) macrocycle PA, c) *o*-Ph-PA, and d) *m*-Ph-PA with increasing ratios of r = [macrocycle]/[DNA]. e) Fluorescence changes of PA (0.01 mM) solution during the gradual addition of DNA. f) Fluorescence displacement assay with G3C3 sequence (1.31×10^{-6} M) and 1 equiv. of EtBr (excitation at 510 nm). The intensity at 600 nm is plotted versus the concentration of the added receptor. Conditions: 50 mM MES 6.2, 140 mM NaCl and 1 mM EDTA (for DNA), 2%DMSO.

it binds the receptors stronger than dodecamers, and we expected stronger CD signals. The changes in the CD spectra of the unsubstituted cyclophane PA were different for those bearing additional phenyl rings (Figure 3 b–d). PA induced strong CD, suggesting the stabilization of the double-stranded DNA, while the addition of o/m-Ph-PA to the DNA solution resulted in a blue shift and a slight increase of ICD. Overall, CD measurements are consistent with the groove binding and intercalation. We found that receptor PA in the presence of DNA shows different fluorescence changes from those observed for the *ortho*- and *meta*-phenyl derivatives. Namely, we observed excimer formation, the intensity of which was maximized at around one receptor per five nucleobase pairs (Figure 3e). This fact suggests that two receptors can fit in the major groove. The excimer formation in the excited state is possible between two receptors via anthracene-anthracene π-π interactions. Anthracene-containing receptors were previously reported to form excimer via DNA binding.[4] To find out if the intercalation mode is present in our systems, we have designed a fluorescence displacement assay based on ethidium bromide (EtBr). The G3T3 sequence solution was treated with EtBr (1 equiv), and then a receptor was added to displace the intercalator. All three receptors were able to displace EtBr from the sequence, resulting in almost complete quenching of EtBr emission (Figure 3f). This behavior suggests that cyclophanes bind to DNA in a similar way as EtBr,[18] i.e. they can intercalate with DNA.

Molecular modeling with subsequent molecular dynamics simulations was conducted to reveal possible binding modes of the receptor molecules *o*-Ph-PA and *m*-Ph-PA with double-stranded DNA (d(GCGAAATTTCGC) and d(CATGGGCCCATG), respectively). As can be seen from the snapshots in Figure 4, both receptors leave the intercalating binding mode of the G3C3 DNA oligomer already after equilibration at finite temperature; however, they 'remain close to the major groove. On the A3T3 DNA oligomers, receptor o-Ph-PA also leaves its intercalating binding site in the course of the simulation. In contrast, receptor m-Ph-PA is observed in an intercalating binding mode throughout the course of the MD simulation. The intercalating moiety is the phenyl ring rather than the anthracene ring system, which is also reflected in the distribution of the distances between the phenyl ring and the central base pair of the DNA (Figure 5a). The phenyl ring exhibits smaller values for *m*-Ph-PA bound to A3T3 DNA than in the other models. Distances to the anthracene ring are comparable (~1.3 nm) in all models, except for *o*-Ph-PA on A3T3 DNA, which shows a higher probability of its anthracene ring being oriented towards the central adenine in the DNA major groove.

Conclusions

In summary, we have synthesized three anthracene-based cyclophanes in which the position of the phenyl substituent was varied. The receptors showed different behavior in binding properties. A strong affinity toward nucleoside triphosphate was observed for the *ortho*-substituted cyclophane. All three receptors showed different degrees of quenching and enhancement with DNA dodecamers. These responses suggest that *m*-Ph-PA has a preference to bind to the GC regions in dsDNA, while PA and *o*-Ph-PA show significant interaction with the central nucleotide regions of sequences and are non-specific. Moreover, PA forms excimers upon excitation at the 1:5 receptor-nucleobase pair ratio. According to molecular

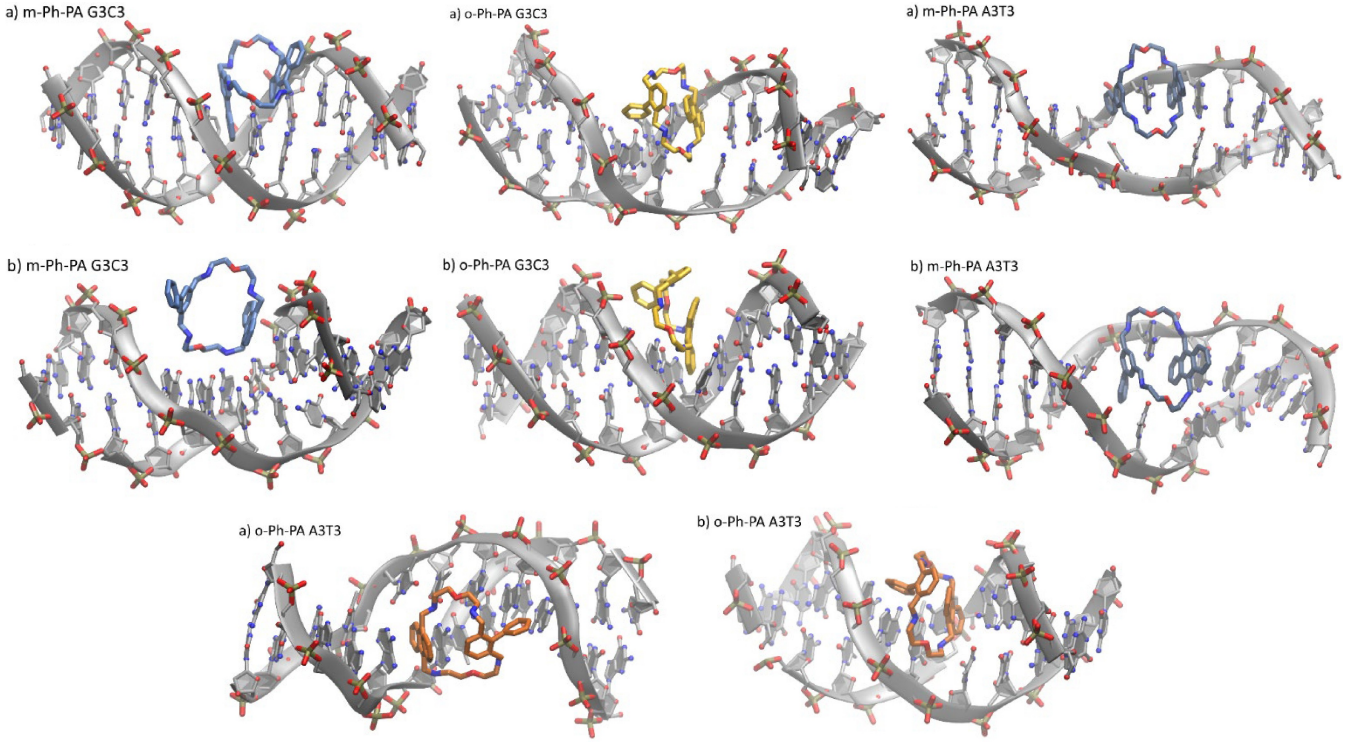

Figure 4. Snapshots of the receptor-DNA complexes after minimization (a) and after equilibration (b) for the G3C3 models and after equilibration (left) and towards the end of the molecular dynamics (MD) simulations (right) for the A3T3 models.

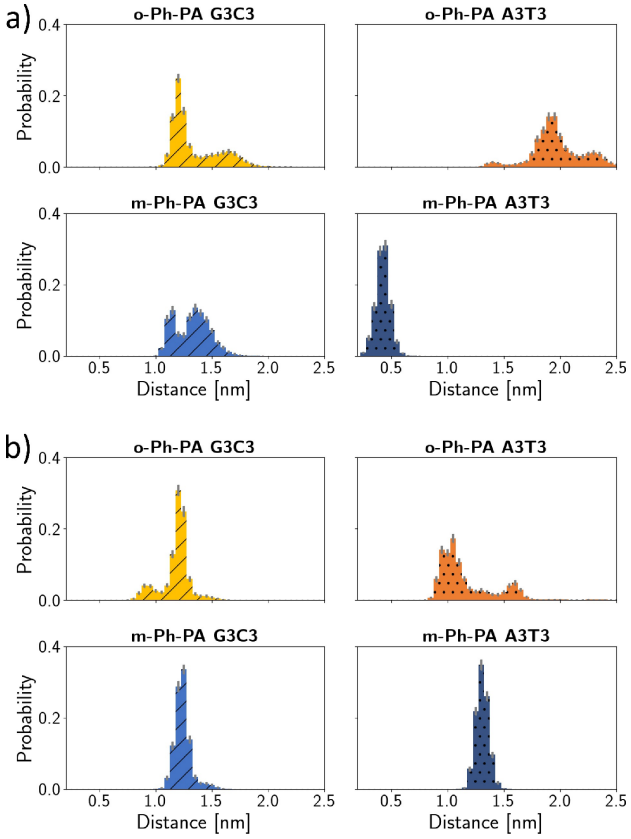

Figure 5. Distribution of distances between the central base pairs of the DNA (A:T to G:C, respectively) and the center of mass of a) the phenyl ring and b) the anthracene ring system of the receptor molecules.

modeling calculations and fluorescence displacement assays with ethidium bromide, the receptor can bind in the major groove or function as an intercalator. The strongest displacement efficiency of ethidium bromide and, thus, better intercalation ability was observed for *m*-Ph-PA. Overall, the obtained data proves the ability of polyammonium cryptands to bind nucleotides and coordinate to double-stranded DNA. We have revealed that the *meta*-phenyl substitution in PA is a promising strategy for designing DNA binders showing GC selectivity and intercalation binding mode. Thus, it would be possible to introduce many fluorescent dyes in the cyclophane structure and hydrogen bond donor and acceptor groups to adjust the binding selectivity. This work is currently in progress.

Experimental Section

Anthracene-9,10-dicarbaldehyde[19] and N-tert-butoxycarbonyl-1,5-diamino-3-oxapentane were prepared according to the published procedures. Di–N-boc-protected 9,10-Bis(7-amino-2-aza-5-oxaheptyl)anthracene was synthesized by a slightly modified procedure reported earlier.[11]

Preparation of PA

A solution of the diamine (127 mg, 0.311 mmol) in the mixture of acetonitrile (94 mL) and MeOH (9.4 mL) was heated at 50 °C under an inert atmosphere. Then, a solution of Isophthalaldehyde (417 mg, 0.311 mmol) in acetonitrile (35 mL) was added dropwise. The reaction mixture was stirred at 50 °C for 72 h. The solvent was removed under reduced pressure without heating. MeOH (100 mL),

DCM (10 mL), and $NaBH_4$ (353 mg, 9.33 mmol) were added sequentially to the residue obtained. The reaction mixture was heated at 50 °C for 3 h, and then it was stirred overnight at RT, followed by the removal of solvent under reduced pressure. The resulting solid was suspended in water (50 mL) and extracted with DCM (3x50 mL). The combined organic phases were dried over Na_2SO_4, and the solvent was removed under reduced pressure. The residue obtained was then purified by column chromatography initially with 50:50 DCM-MeOH to remove all the impurity spots, followed by 50:50:0.5 DCM-MeOH-NH_3 and then with 50:50:1 DCM-MeOH-NH_3 to obtain the product in 33% yield (52 mg, 0.1014 mmol). ^{1}H NMR (400 MHz, $CDCl_3$): δ[ppm] = 2.72 (t, J = 6 Hz, 4H), 3.04 (t, J = 4 Hz. 4H), 3.49 (s, 4H), 3.53 (t, J = 6 Hz, 4H), 3.64 (t, J = 4 Hz, 4H), 4.72 (s, 4H), 6.76 (s, 1H), 7.14 (d, 3H), 7.36–7.39 (m, 4H), 8.31–8.34 (m, 4H). ^{13}C NMR (400 MHz, $CDCl_3$): δ [ppm] = 45.68, 49.47, 49.69, 53.97, 69.83, 70.23, 124.82, 125.96, 127.24, 128.02, 128.42, 130.12, 132.10, 139.84. HRMS (ESI) Calcd for $C_{32}H_{41}N_4O_2$ $[M+H]^+$: m/z = 513.3224, found: m/z = 513.3233; calcd for $C_{32}H_{41}N_4O_2$ $[M+2H]^{2+}$: m/z = 297.1191, found: m/z = 297.1120.

Preparation of *o*-Ph-PA

A solution of the corresponding diamine (507 mg, 1.236 mmol) in acetonitrile (373 mL) and MeOH (37 mL) was heated at 50 °C under inert atmosphere. Then, a solution of the dialdehyde (260 mg, 1.236 mmol) in acetonitrile (125 mL) was added dropwise. The reaction mixture was stirred at room temperature for 72 h. Then, the solvent was removed under reduced pressure without heating. To the residue obtained, MeOH (200 mL) and DCM (20 mL) and $NaBH_4$ (1402.7 mg, 37.08 mmol) were added. The reaction mixture was heated at 50 °C for 3 h, then the reaction mixture was stirred overnight at RT, and the solvent was removed under reduced pressure. The resulting solid was suspended in water (50 mL) and then extracted with DCM (3x50 mL). The combined organic phases were dried over Na_2SO_4, and the solvent was removed under reduced pressure. The residue obtained was then purified by column chromatography initially with 50:50 DCM-MeOH to remove all the impurity spots, followed by 100:100:0.5 DCM-MeOH-NH_3 and then with 100:100:1 DCM-MeOH-NH_3 to obtain the product (35 mg, 0.059 mmol, 20%). ^{1}H NMR (400 MHz, $CDCl_3$): δ[ppm] = 2.49 (t, J = 4 Hz, 4H), 3.01 (t, J = 6 Hz, 4H), 3.22 (s, 4H), 3.39 (t, J = 6 Hz, 4H), 3.56 (t, J = 6 Hz, 4H), 4.71 (s, 4H), 6.48 (d, J = 8 Hz, 2H), 6.73 (t, J = 8 Hz, 2H), 6.90 (t, J = 8 Hz, 1H), 7.11 (t, J = 8 Hz, 1H), 7.27 (d, J = 8 Hz, 2H), 7.34–7.37 (m, 4H), 8.31–8.35 (m, 4H). ^{13}C NMR (400 MHz, $CDCl_3$): δ[ppm] = 44.55, 48.35, 48.57, 50.85, 68.57, 69.39, 123.75, 124.98, 126.03, 126.53, 126.87, 127.05, 127.60, 129.10, 131.11, 136.93, 137.34, 139.82. HRMS (ESI) Calcd for $C_{38}H_{45}N_4O_2$ $[M+H]^+$: m/z = 589.3537, found: m/z = 589.3536; Calcd for $C_{38}H_{46}N_4O_2$ $[M+2H]^{2+}$: m/z = 295.1805, found: m/z = 295.1816.

Preparation of *m*-Ph-PA

A solution of the diamine (100 mg, 0.244 mmol) in acetonitrile (150 mL) and MeOH (12 mL) was heated at 50 °C under an inert atmosphere. Then, a solution of the corresponding dialdehyde (51 mg, 0.244 mmol) in acetonitrile (100 mL) was added dropwise. The reaction mixture was stirred at the same temperature for 72 h. Then, the solvent was removed under reduced pressure without heating. MeOH (200 mL), DCM (20 mL) and NaBH4 (700.3 mg, 17.5 mmol) were added subsequently to the residue obtained. The reaction mixture was heated at 50 °C for 3 h, then the reaction mixture was stirred overnight at RT, and the solvent was removed under reduced pressure. The resulting solid is suspended in water (50 mL) and then extracted with DCM (3x50 mL). The combined organic phase was dried over Na_2SO_4, and the solvent was removed under reduced pressure. The residue obtained was then purified by column chromatography initially with ethanol-THF 1:1 and then with ethanol-THF-ammonia 100:100:5., to obtain the macrocycle as a pale yellow oil in 21% yield. (30 mg, 0.055 mmol). ^{1}H NMR (600 MHz, $CDCl_3$) δ 8.32 (m, 4H), 7.60 (d, 2H), 7.44 (s, 2H), 7.41 (d, 2H), 7.36 (m, 4H), 7.32 (t, 2H), 4.71 (s, 4H), 3.65 (m, 4H), 3.55 (s, 4H), 3.53 (m, 4H), 3.05 (m, 4H), 2.77 (m, 4H). ^{13}C NMR (151 MHz, $CDCl_3$) δ 140.3, 140.0, 139.3, 131.0, 129.0, 127.8, 126.40, 126.3, 126.1, 125.0, 124.9, 123.7, 69.1, 68.8, 53.1, 48.6, 48.5, 44.5. HRMS (ESI) Calcd for $C_{38}H_{45}N_4O_2$ $[M+H]^+$: m/z = 589.3537, found: m/z = 589.3539; Calcd for $C_{38}H_{46}N_4O_2$ $[M+2H]^{2+}$: m/z = 295.1805, found: m/z = 295.1813.

Molecular Modeling Calculations

We have built models of DNA oligomer GCGAAATTTCGCG and CATGGGCCCATG, both with intercalator molecules *m*-Ph-PA and *o*-Ph-PA bound, respectively. The DNA oligomers were modeled as B-DNA using the webserver 3DNA. The intercalator molecules were placed on the DNA manually, creating an intercalating pose for which the central DNA bases were slightly displaced so as to accommodate the Ph-PA molecules. (This was necessary since docking of the receptor molecules to the unperturbed B-DNA using Autodck[20] did not result in an intercalating pose. The docking poses are shown as supplementary material). All models were solvated in TIP3 water[21] in a truncated octahedral box- large enough to allow 1.5 nm between solvent and the edge of the box. Na^+ ions were added to neutralize the systems, and additional NaCl was added to reach a 0.15 mol/L salt concentration. Periodic boundary conditions and a particle-mesh Ewald[22] treatment for the long-range electrostatic (0.16 nm grid spacing, interpolation to 4th order) were employed with a cut-off of 1.4 nm for both short-range electrostatics and van-der-Waals interactions. All covalent bonds to hydrogen atoms were kept stationary using the LINCS algorithm,[23] thus allowing an integration time step of 2 fs. The systems were simulated in an NVT ensemble; temperature was controlled by canonical sampling through velocity rescaling (V-rescale[24]) with a time constant of 0.1 ps. Simulations were performed at 300 K. During an equilibration period of 0.2 ns all solute heavy atoms were restrained. From the production runs of 1 μs, the first 200 ns were not included in the subsequent analysis, considering this as a further equilibration phase. All molecular dynamics simulations have been performed using the Gromacs package.[25] The DNA was described by the amber parmBSC1 force field,[26] the intercalator molecule by a GAFF force field[27] with customized parameters. Analyses were carried out with Gromacs tools, visualization of molecules are generated using VMD,[28] plots have been generated with matplotlib.[29]

Acknowledgements

Financial support for this work was provided by DFG grants KA 3444/16-1 and KA 3444/25-1. We also thank FAU Erlangen-Nürnberg and the Philipp Schwartz Initiative of the Alexander von Humboldt Foundation for supporting Ismet Basaran. Open Access funding enabled and organized by Projekt DEAL.

Conflict of Interests

The authors declare no conflict of interest.

Data Availability Statement

The data that support the findings of this study are available in the supplementary material of this article.

Keywords: Cyclophanes · Fluorescence sensing · Nucleotide · Recognition · π–π interaction

[1] a) H. Ihmels, D. Otto, *Supermolecular Dye Chemistry* **2005**, *258*, 161–204; b) E. Pazos, J. Mosquera, M. E. Vazquez, J. L. Mascarenas, *Chembiochem.* **2011**, *12*, 1958–1973; c) P. B. Dervan, *Bioorgan. Med. Chem.* **2001**, *9*, 2215–2235; d) S. C. Zimmerman, *Beilstein J. Org. Chem.* **2016**, *12*, 125–138.
[2] a) D. Ramaiah, P. P. Neelakandan, A. K. Nair, R. R. Avirah, *Chem. Soc. Rev.* **2010**, *39*, 4158–4168; b) A. M. Agafontsev, A. Ravi, T. A. Shumilova, A. S. Oshchepkov, E. A. Kataev, *Chem-Eur. J.* **2019**, *25*, 2684–2694; c) Y. Zhou, Z. Xu, J. Yoon, *Chem. Soc. Rev.* **2011**, *40*, 2222–2235; d) I. Piantanida, B. S. Palm, P. Cudic, M. Zinic, H.-J. Schneider, *Tetrahedron Lett.* **2001**, *42*, 6779–6783; e) H. Zhang, L. Cheng, H. Nian, J. Du, T. Chen, L. Cao, *Chem. Commun.* **2021**, *57*, 3135–3138; f) A. M. Agafontsev, T. A. Shumilova, A. S. Oshchepkov, F. Hampel, E. A. Kataev, *Chem. – Eur. J.* **2020**, *26*, 9991–9997; g) A. M. Agafontsev, T. A. Shumilova, T. Rüffer, H. Lang, E. A. Kataev, *Chem. – Eur. J.* **2019**, *25*, 3541–3549.
[3] a) O. Baudoin, F. Gonnet, M. P. Teulade-Fichou, J. P. Vigneron, J. C. Tabet, J. M. Lehn, *Chem.-Eur. J.* **1999**, *5*, 2762–2771b) P. Cudic, M. Zinic, V. Tomisic, V. Simeon, J. P. Vigneron, J. M. Lehn, *J. Chem. Soc. Chem. Comm.* **1995**, 1073–1075; c) P. P. Neelakandan, M. Hariharan, D. Ramaiah, *J. Am. Chem. Soc.* **2006**, *128*, 11334–11335.
[4] P. P. Neelakandan, D. Ramaiah, *Angew. Chem. Int. Ed.* **2008**, *47*, 8407–8411.
[5] B. S. Morozov, A. S. Oshchepkov, I. Klemt, A. M. Agafontsev, S. Krishna, F. Hampel, H.-G. Xu, A. Mokhir, D. Guldi, E. Kataev, *JACS Au.* **2023**, *3*, 964–977.
[6] a) M. Jourdan, J. Garcia, J. Lhomme, M. P. Teulade-Fichou, J. P. Vigneron, J. M. Lehn, *Biochemistry* **1999**, *38*, 14205–14213; b) A. Granzhan, N. Kotera, M. P. Teulade-Fichou, *Chem. Soc. Rev.* **2014**, *43*, 3630–3665; c) K. Nakatani, *B. Chem. Soc. Jpn.* **2009**, *82*, 1055–1069.
[7] a) Y. Chu, D. W. Hoffman, B. L. Iverson, *J. Am. Chem. Soc.* **2009**, *131*, 3499–3508; b) J. M. Veal, Y. Li, S. C. Zimmerman, C. R. Lamberson, M. Cory, G. Zon, W. D. Wilson, *Biochemistry* **1990**, *29*, 10918–10927; c) S. C. Zimmerman, C. R. Lamberson, M. Cory, T. A. Fairley, *J. Am. Chem. Soc.* **1989**, *111*, 6805–6809; d) P. Guo, A. A. Farahat, A. Paul, D. W. Boykin, W. D. Wilson, *Chem. Sci.* **2021**, *12*, 15849–15861.
[8] W. B. Tan, A. Bhambhani, M. R. Duff, A. Rodger, C. V. Kumar, *Photochem. Photobiol.* **2006**, *82*, 20–30.
[9] M. R. Duff, V. K. Mudhivarthi, C. V. Kumar, *J. Phys. Chem. B* **2009**, *113*, 1710–1721.
[10] a) A. Granzhan, M. P. Teulade-Fichou, *Chem.-Eur. J.* **2009**, *15*, 1314–1318; b) M. Bahr, V. Gabelica, A. Granzhan, M.-P. Teulade-Fichou, E. Weinhold, *Nucleic Acids Res.* **2008**, *36*, 5000–5012; c) N. Kotera, A. Granzhan, M.-P. Teulade-Fichou, *Biochimie* **2016**, *128–129*, 133–137; d) M. Jourdan, A. Granzhan, R. Guillot, P. Dumy, M. P. Teulade-Fichou, *Nucleic Acids Res.* **2012**, *40*, 5115–5128.
[11] A. Granzhan, E. Largy, N. Saettel, M. P. Teulade-Fichou, *Chem.-Eur. J.* **2010**, *16*, 878–889.
[12] J. Schlosser, J. F. M. Hebborn, D. V. Berdnikova, H. Ihmels, *Chemistry* **2023**, *5*, 1220–1232.
[13] D. Christopher Braddock, T. Cailleau, G. Cansell, S. A. Hermitage, R. H. Pouwer, J. M. Redmond, A. J. P. White, *Tetrahedron Asymm.* **2010**, *21*, 2911–2919.
[14] a) F. Neese, *Wires Comput Mol Sci* **2012**, *2*, 73–78; b) F. Neese, *Wires Comput Mol Sci* **2022**, *12*, e1606.
[15] a) S. Grimme, S. Ehrlich, L. Goerigk, *J. Comput. Chem.* **2011**, *32*, 1456–1465; b) S. Grimme, J. Antony, S. Ehrlich, H. Krieg, *J. Chem. Phys.* **2010**, *132*, 154104.
[16] A. V. Marenich, C. J. Cramer, D. G. Truhlar, *J. Phys. Chem. B* **2009**, *113*, 6378–6396.
[17] N. A. Corfu, H. Sigel, *Eur. J. Biochem.* **1991**, *199*, 659–669.
[18] S. Nafisi, A. A. Saboury, N. Keramat, J.-F. Neault, H.-A. Tajmir-Riahi, *J. Mol. Struct.* **2007**, *827*, 35–43.
[19] A. Slodek, M. Filapek, E. Schab-Balcerzak, M. Grucela, S. Kotowicz, H. Janeczek, K. Smolarek, S. Mackowski, J. G. Malecki, A. Jedrzejowska, G. Szafraniec-Gorol, A. Chrobok, B. Marcol, S. Krompiec, M. Matussek, *Eur. J. Org. Chem.* **2016**, *2016*, 4020–4031.
[20] G. M. Morris, R. Huey, W. Lindstrom, M. F. Sanner, R. K. Belew, D. S. Goodsell, A. J. Olson, *J. Comput. Chem.* **2009**, *30*, 2785–2791.
[21] W. L. Jorgensen, J. Chandrasekhar, J. D. Madura, R. W. Impey, M. L. Klein, *J. Chem. Phys.* **1983**, *79*, 926–935.
[22] T. Darden, D. York, L. Pedersen, *J. Chem. Phys.* **1993**, *98*, 10089–10092.
[23] B. Hess, H. Bekker, H. J. C. Berendsen, J. G. E. M. Fraaije, *J. Comput. Chem.* **1997**, *18*, 1463–1472.
[24] G. Bussi, D. Donadio, M. Parrinello, *J. Chem. Phys.* **2007**, *126*, 014101.
[25] D. Van Der Spoel, E. Lindahl, B. Hess, G. Groenhof, A. E. Mark, H. J. C. Berendsen, *J. Comput. Chem.* **2005**, *26*, 1701–1718.
[26] I. Ivani, P. D. Dans, A. Noy, A. Pérez, I. Faustino, A. Hospital, J. Walther, P. Andrio, R. Goñi, A. Balaceanu, G. Portella, F. Battistini, J. L. Gelpí, C. González, M. Vendruscolo, C. A. Laughton, S. A. Harris, D. A. Case, M. Orozco, *Nat. Methods* **2016**, *13*, 55-++.
[27] J. M. Wang, R. M. Wolf, J. W. Caldwell, P. A. Kollman, D. A. Case, *J. Comput. Chem.* **2004**, *25*, 1157–1174.
[28] W. Humphrey, A. Dalke, K. Schulten, *J. Mol. Graph Model* **1996**, *14*, 33–38.
[29] J. D. Hunter, *Comput. Sci. Eng.* **2007**, *9*, 90–95.

Manuscript received: May 30, 2024
Accepted manuscript online: August 7, 2024
Version of record online: October 2, 2024